Available online at www.sciencedirect.com
ScienceDirect
Polymer 48 (2007) 467–476
polymer
www.elsevier.com/locate/polymer

Synthesis and properties of helical polyacetylenes containing carbazole

Jinqing Qu, Ritsuya Kawasaki, Masashi Shiotsuki, Fumio Sanda*, Toshio Masuda*

Department of Polymer Chemistry, Graduate School of Engineering, Kyoto University, Katsura Campus, Kyoto 615-8510, Japan

Received 28 August 2006; received in revised form 20 November 2006; accepted 21 November 2006
Available online 13 December 2006

Abstract

Novel acetylene monomers containing carbazole with chiral menthyl and bornyl groups, 9-(1*R*,2*S*,5*R*)-menthyloxycarbonyl-2-ethynylcarbazole (**1**), 9-(1*S*,2*R*,5*S*)-menthyloxycarbonyl-2-ethynylcarbazole (**2**), 9-(1*R*,2*S*,5*R*)-menthyloxycarbonyl-3-ethynylcarbazole (**3**) and 9-(1*S*)-bornyloxycarbonyl-2-ethynylcarbazole (**4**) were synthesized and polymerized with a Rh catalyst to give the corresponding polymers [poly(**1**)–poly(**4**)] with moderate M_n value of $(11.5–92.2) \times 10^3$ in good yields (77–89%). CD spectroscopic studies revealed that poly(**1**), poly(**2**) and poly(**4**) took predominantly one-handed helical structure in $CHCl_3$, THF, toluene, and CH_2Cl_2, while poly(**3**) did not. Addition of methanol to $CHCl_3$ solutions of poly(**1**) and poly(**2**) resulted in the formation of aggregates showing smaller CD signals at 275 and 320 nm. The helical structure of poly(**1**) and poly(**2**) was very stable against heating. The polymers emitted fluorescence in 0.40–2.90% quantum yields. Poly(**4**) exhibited an obvious oxidation peak at 1.10 V. The polymers were thermally stable below 300 °C.

Keywords: Carbazole; Helical polymers; Polyacetylenes

1. Introduction

Carbazole is widely used as hole-transporting and electroluminescent units. Polymers containing carbazole moieties in the main chain or side chain have attracted much attention because of their unique properties, which allow them to be applied to various photonic materials such as photoconductive, electroluminescent, and photorefractive materials [1]. Meanwhile, substituted polyacetylenes exhibit unique properties such as semiconductivity, high gas permeability, and nonlinear optical properties [2]. Polyacetylenes with appropriate substituents form helices. Helical polymers gather interest not only from the view point of synthesis and properties [3], but also from practical application, because they exhibit useful functions based on the secondary structure, including chiral discrimination and catalytic activity for asymmetric synthesis [4]. *cis*-Stereoregular helical polyacetylenes are commonly prepared by the polymerization of chiral monomers using Rh catalysts, which include poly(phenylacetylenes) carrying menthyl group, phenethyl group, and amino acid [5–7], some of which exhibit unique properties such as self-assembling, formation of superhelical fibers, chirality transcription, and tuning the helicity upon external stimuli. We have synthesized a series of helical poly(propiolic esters), poly(propargyl esters), poly(*N*-propargylamides), poly(*N*-propargylcarbamates), and poly(*N*-butynylamides) having various chiral pendant groups [8]. Among them, hydroxy- and amide-containing polymers stabilize the helical structures with intramolecular hydrogen bonds as well as steric repulsion between the side chains. Therefore, they undergo transition from helix to random coil and/or helix inversion according to the change in polarity of solvents.

Incorporation of carbazole into polyacetylenes possibly leads to the development of novel functional polymers based on synergistic actions of carbazole and main chain conjugation [9–11]. The drawback of carbazole-containing polyacetylenes is poor solubility in solvents, which makes the elucidation of their properties difficult. One solution to this issue is

* Corresponding authors. Tel.: +81 75 383 2589; fax: +81 75 383 2590 (T.M.).
E-mail addresses: sanda@adv.polym.kyoto-u.ac.jp (F. Sanda), masuda@adv.polym.kyoto-u.ac.jp (T. Masuda).

0032-3861/$ - see front matter © 2006 Elsevier Ltd. All rights reserved.
doi:10.1016/j.polymer.2006.11.042

incorporation of a flexible spacer between polyacetylene backbone and carbazole moiety [12]. We have recently found that transformation of NH of carbazole into NCOOR effectively enhances the solubility of carbazole-containing polyacetylenes, even when polyacetylene backbone is directly connected with carbazole at the benzene ring [13]. Adopting a chiral group to NCOOR enables us to obtain a chiral polyacetylene carrying carbazole, which possibly takes a helical structure. This polymer may form a helical carbazole strand as well as a helical polyacetylene main chain, leading to unique electronic and photonic functions besides chiroptical properties. The synthesis and secondary structure of this type of polymers have been scarcely investigated to the best of our knowledge [14]. The present study deals with the synthesis and polymerization of carbazole-based novel acetylene monomers **1**–**4** with optically active carbamate moieties derived from (1*R*,2*S*,5*R*)-(−)-menthol, (1*S*,2*R*,5*S*)-(+)-menthol, and (1*S*)-endo-(−)-borneol (Scheme 1), and examination of the optical and electrochemical properties.

2. Experimental section

2.1. Measurements

^{1}H (400 MHz) and ^{13}C (100 MHz) NMR spectra were recorded on a JEOL EX-400 spectrometer using tetramethylsilane as an internal standard. IR, UV–vis, and fluorescence spectra were measured on JASCO FT/IR-4100, V-550, and FP750 spectrophotometers, respectively. Melting points (mp) were measured on a Yanaco micro melting point apparatus. Elemental analysis was carried out at the Kyoto University Elemental Analysis Center. The number- and weight-average molecular weights (M_n and M_w) of polymers were determined by gel permeation chromatography (GPC) on a JASCO GULLIVER system (PU-980, CO-965, RI-930, and UV-1570) equipped with polystyrene gel columns (Shodex columns K804, K805, and J806) using tetrahydrofuran (THF) as an eluent at a flow rate of 1.0 mL/min, calibrated by polystyrene standards at 40 °C. Cyclic voltammograms were measured on an HCH Instruments ALS600A-n electrochemical analyzer. The measurements were carried out with a glassy carbon rod as the working electrode coupled with a Pt plate counter electrode and a Ag/AgCl reference electrode, with a solution of a polymer (1 mM) and tetrabutylammonium perchlorate (TBAP, 0.1 M) in CH_2Cl_2. Thermal gravimetric analysis (TGA) was carried out with a Perkin–Elmer TGA-7 thermal analyzer.

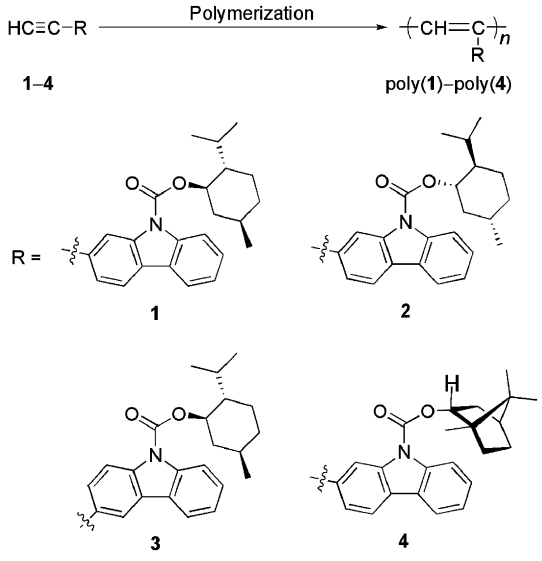

Scheme 1. Polymerization of **1**–**4**.

2.2. Materials

Unless otherwise stated, reagents were purchased and used without purification. 2- and 3-trimethylsilylethynylcarbazoles were synthesized according to the literature [13]. Solvents for polymerization were purified before use by the standard methods.

2.3. Monomer synthesis

Monomers **1**–**4** containing carbazole moieties with different chiral groups were synthesized by the routes illustrated in Scheme 2. The experimental procedures for the synthesis of 9-(1*R*,2*S*,5*R*)-menthyloxycarbonyl-2-ethynylcarbazole (**1**) are given below as examples.

A 200 mL three-necked flask was equipped with a three-way stopcock and a magnetic stirring bar, and filled with dry nitrogen. A solution of (1*R*,2*S*,5*R*)-(−)-menthol (1.8 g, 12 mmol) in THF (15 mL) was added to a solution of triphosgene (1.3 g, 4.0 mmol) in THF (30 mL). After stirring the mixture for 15 min, a solution of Et_3N (1.6 mL, 12 mmol) in THF (10 mL) was slowly added to the mixture, and the resulting mixture was stirred at room temperature overnight. Solvent-insoluble salt was filtered off to obtain a solution of (1*R*,2*S*,5*R*)-menthyl chloroformate. The solution of crude (1*R*,2*S*,5*R*)-menthyl chloroformate was slowly added to a solution of 2-trimethylsilylethynylcarbazole (1.5 g, 5.7 mmol) in THF (20 mL) and Et_3N (2.0 mL, 14 mmol). After stirring for 8 h at 60 °C, the reaction mixture was stirred at room temperature overnight. The resulting solution was filtered, and the filtrate was concentrated with a rotary evaporator. Purification of the crude product by silica gel column chromatography eluted with *n*-hexane/ethyl acetate = 9/1 (volume ratio) provided 9-(1*R*,2*S*,5*R*)-menthyloxycarbonyl-2-trimethylsilylethynylcarbazole as a pale yellow solid. Yield 1.0 g (39%).

A 100 mL three-necked flask was equipped with a three-way stopcock and a magnetic stirring bar, and filled with dry nitrogen. A solution of tetrabutylammonium fluoride (TBAF, 1 M THF solution) (2.3 mL, 2.3 mmol) in THF (5 mL) was added to a solution of 9-(1*R*,2*S*,5*R*)-menthyloxycarbonyl-2-trimethylsilylethynylcarbazole (1.0 g, 2.2 mmol) in THF (15 mL), and the mixture was stirred for 5 min at room temperature, then the reaction mixture was diluted with $CHCl_3$ (30 mL). The solution was washed subsequently with aq. NH_4Cl, brine and water. The organic layer was dried over anhydrous $MgSO_4$ and concentrated to afford a pale yellow

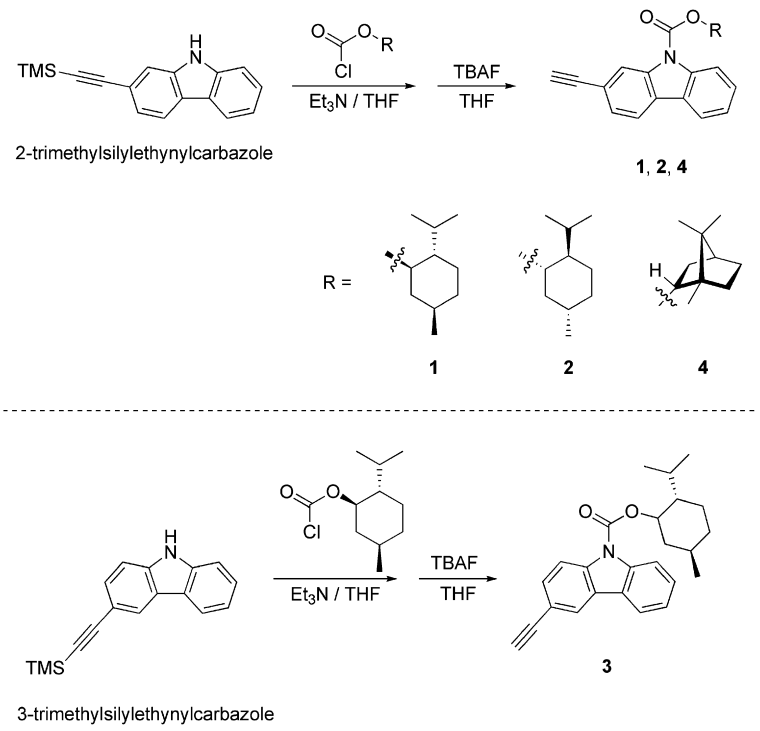

Scheme 2. Synthetic routes of **1**–**4**.

solid. It was purified by silica gel column chromatography eluted with *n*-hexane/ethyl acetate 9/1 (volume ratio) to afford **1** as a white solid. Yield 0.55 g (66%), mp = 47–48 °C. $[\alpha]_D = -109°$ ($c = 0.1$ g/dL in $CHCl_3$). ^{1}H NMR (δ in ppm, $CDCl_3$): 0.77 (d, $J = 6.8$ Hz, 3H, CH*Me*), 0.90 (d, $J = 6.8$ Hz, 6H, CH*Me*$_2$), 1.10–1.74 (m, 7H, C*H*$_2$C*H*MeC*H*$_2$C*H*$_2$), 2.01–2.06 (m, 1H, Me$_2$C*H*), 2.22–2.25 (m, 1H, C*H*CHMe$_2$), 3.06 (s, 1H, C≡CH), 4.99–5.02 (m, 1H, OC*H*), 7.26 (vt, $J =$ 3.8 Hz, 1H, Ar), 7.40–7.42 (m, 2H, Ar), 7.82 (d, $J = 8.8$ Hz, 1H, Ar), 7.87 (d, $J = 8.0$ Hz, 1H, Ar), 8.22 (d, $J = 8.0$ Hz, 1H, Ar), 8.41 (s, 1H, Ar). ^{13}C NMR (δ in ppm, $CDCl_3$): 16.4, 20.9, 22.0, 23.5, 26.4, 31.6, 34.1, 41.2, 47.4, 78.0 (C≡*C*H), 84.4 (*C*≡CH), 116.4, 119.4, 119.9, 120.3, 120.5, 123.4, 125.2, 126.2, 127.1, 127.7, 137.9, 138.9, 151.9 (CO_2). IR (cm^{-1}, KBr): 3291 (≡C–H), 2105 (C≡C), 2956, 2869, 1725, 1601, 1493, 1456, 1425, 1370, 1330, 1304, 1278, 1257, 1220, 1203, 1118, 1096, 1037, 988, 947, 823, 763, 747, 723. Anal. Calcd for $C_{25}H_{27}NO_2$: C 80.40, H 7.29, N 3.75. Found: C 80.01, H 7.24, N 3.47.

Other monomers were synthesized by the procedures similar to those described above for the preparation of monomer **1**. Their characterization data are given below. 9-(1*S*,2*R*,5*S*)-Menthyloxycarbonyl-2-ethynylcarbazole (**2**): pale yellow solid. 40% yield, mp = 49–50 °C. $[\alpha]_D = +109°$ ($c = 0.1$ g/dL in $CHCl_3$). ^{1}H NMR (δ in ppm, $CDCl_3$): 0.77 (d, $J = 6.8$ Hz, 3H, CH*Me*), 0.90 (d, $J = 6.8$ Hz, 6H CH*Me*$_2$), 1.10–1.74 (m, 7H, C*H*$_2$C*H*MeC*H*$_2$C*H*$_2$), 2.01–2.06 (m, 1H, Me$_2$C*H*), 2.22–2.25 (m, 1H, C*H*CHMe$_2$), 3.06 (s, 1H, C≡CH), 4.99–5.02 (m, 1H, OC*H*), 7.26 (vt, $J = 3.8$ Hz, 1H, Ar), 7.40–7.42 (m, 2H, Ar), 7.82 (d, $J = 8.8$ Hz, 1H, Ar), 7.87 (d, $J = 8.0$ Hz, 1H, Ar), 8.22 (d, $J = 8.0$ Hz, 1H, Ar), 8.41 (s, 1H, Ar). ^{13}C NMR (δ in ppm, $CDCl_3$): 16.2, 20.8, 22.0, 23.4, 26.4, 31.5, 34.1, 41.2, 47.4, 78.0 (C≡*C*H), 84.4 (*C*≡CH), 116.4, 119.4, 119.9, 120.3, 120.5, 123.4, 125.2, 126.2, 127.1, 127.7, 137.9, 138.9, 151.9 (CO_2). IR (cm^{-1}, KBr): 3293 (≡C–H), 2105 (C≡C), 2956, 2868, 1725, 1600, 1492, 1455, 1425, 1370, 1330, 1306, 1278, 1256, 1202, 1149, 1130, 1118, 1096, 1037, 988, 945, 823, 763, 747, 723. Anal. Calcd for $C_{25}H_{27}NO_2$: C 80.40, H 7.29, N 3.75. Found: C 80.22, H 7.31, N 3.65. 9-(1*R*,2*S*,5*R*)-Menthyloxycarbonyl-3-ethynylcarbazole (**3**): pale yellow solid. 40% yield, mp = 58–59 °C. $[\alpha]_D = -99°$ ($c = 0.1$ g/dL in $CHCl_3$). ^{1}H NMR (δ in ppm, $CDCl_3$): 0.77 (d, $J = 6.8$ Hz, 3H, CH*Me*), 0.81–0.89 (m, 6H, CH*Me*$_2$), 1.00–1.74 (m, 7H, C*H*$_2$C*H*MeC*H*$_2$C*H*$_2$), 1.98–2.05 (m, 1H, Me$_2$C*H*), 2.20–2.22 (m, 1H, C*H*CHMe$_2$), 3.03 (s, 1H, C≡CH), 4.97–5.01 (m, 1H, OC*H*), 7.25–8.22 (m, 7H, Ar). ^{13}C NMR (δ in ppm, $CDCl_3$): 16.3, 20.9, 22.0, 23.4, 26.4, 31.5, 34.1, 41.2, 47.4, 78.0 (C≡*C*H), 83.5 (*C*≡CH), 116.4, 116.7, 117.1, 119.7, 123.5, 123.6, 125.1, 125.9, 127.7, 131.5, 138.3, 138.7, 151.9 (CO_2). IR (cm^{-1}, KBr): 3290 (≡C–H), 2107 (C≡C), 2956, 2869, 1727, 1603, 1493, 1450, 1425, 1370, 1300, 1253, 1220, 1149, 1134, 1118, 1096, 1034, 967, 932, 824, 763, 747, 727. Anal. Calcd for $C_{25}H_{27}NO_2$: C 80.40, H 7.29, N 3.75. Found: C 80.11, H 7.29, N 3.55. 9-(1*S*)-Bornyloxycarbonyl-2-ethynylcarbazole (**4**): pale yellow solid. 40% yield, mp = 42–43 °C. $[\alpha]_D = -4°$ ($c = 0.1$ g/dL in $CHCl_3$). ^{1}H NMR (δ in ppm, $CDCl_3$): 0.96 (s, 3H, Me), 1.02 (s, 3H, Me), 1.05 (s, 3H, Me), 1.36–1.42 (m, 2H, CH_2), 1.50–1.60 (m, 1H, CH_2), 1.81–1.90 (m, 2H, CH_2), 2.12–2.20 (m, 1H, CH_2), 2.57–2.65 (m, 1H, CH_2), 3.13 (s, 1H, C≡CH), 5.32–5.34 (m, 1H, OC*H*), 7.35 (vt, $J = 3.8$ Hz, 1H, Ar),

7.49–7.51 (m, 2H, Ar), 7.88 (d, $J = 8.4$ Hz, 1H, Ar), 7.93 (d, $J = 7.6$ Hz, 1H, Ar), 8.32 (d, $J = 8.4$ Hz, 1H, Ar), 8.53 (s, 1H, Ar). ^{13}C NMR (δ in ppm, $CDCl_3$): 13.6, 18.9, 19.8, 27.9, 28.1, 36.87, 44.7, 48.1, 49.1, 78.0 (C≡*C*H), 84.4 (*C*≡CH), 116.2, 119.4, 119.9, 120.3, 120.5, 123.4, 125.3, 126.2, 127.1, 127.7, 137.9, 138.9 (Ar), 152.6 (CO_2). IR (cm^{-1}, KBr): 3290 (≡C–H), 2103 (C≡C), 2954, 2869, 1726, 1601, 1491, 1466, 1456, 1425, 1386, 1352, 1331, 1306, 1278, 1255, 1220, 1203, 1148, 1130, 1114, 1042, 991, 966, 887, 822, 768, 746, 722. Anal. Calcd for $C_{25}H_{25}NO_2$: C 80.83, H 6.78, N 3.77. Found: C 80.48, H 6.84, N 3.53.

2.4. Polymerization

All the polymerizations were carried out in a Schlenk tube equipped with a three-way stopcock under dry nitrogen. A CH_2Cl_2 solution of a monomer ($[M]_{total} = 0.1$ M) was added to a CH_2Cl_2 solution of (nbd)$Rh^+[\eta^6$-$C_6H_5B^-(C_6H_5)_3]$ ([monomer]/[cat] = 100) under dry nitrogen, and the solution was kept at 30 °C for 24 h. The polymerization mixture was poured into a large amount of acetone to precipitate a polymer. It was separated from the supernatant by filtration and dried under reduced pressure.

2.5. Spectroscopic data of the polymers

Poly(**1**): ^{1}H NMR (δ in ppm, $CDCl_3$): 0.8–2.4 (br, 18H), 5.1 (br, 1H, OC*H*), 5.9 (br, 1H, C=CH), 6.3–8.6 (br, 7H, Ar). IR (cm^{-1}, KBr): 3430, 3055, 2954, 2866, 1720, 1600, 1493, 1456, 1421, 1370, 1330, 1259, 1203, 1118, 1034, 983, 881, 823, 761, 744, 724. Poly(**2**): ^{1}H NMR (δ in ppm, $CDCl_3$): 0.8–2.4 (br, 18H), 5.1 (br, 1H, OC*H*), 5.9 (br, 1H, C=CH), 6.3–8.6 (br, 7H, Ar). IR (cm^{-1}, KBr): 3435, 3055, 2955, 2866, 1724, 1600, 1493, 1456, 1421, 1370, 1331, 1259, 1202, 1118, 1034, 983, 881, 811, 761, 743, 723. Poly(**3**): ^{1}H NMR (δ in ppm, $CDCl_3$): 0.9–2.2 (br, 18H, menthyl), 5.1 (br, 1H, OC*H*), 5.9 (br, 1H, C=CH), 6.3–8.4 (br, 7H, Ar). IR (cm^{-1}, KBr): 3437, 3046, 2954, 2866, 1728, 1602, 1493, 1451, 1421, 1370, 1330, 1259, 1203, 1118, 1034, 983, 881, 823, 761, 744, 724. Poly(**4**): ^{1}H NMR (δ in ppm, $CDCl_3$): 0.9–2.7 (br, 16H), 5.0 (br, 1H, OC*H*), 6.0 (br, 1H, C=CH), 6.3–8.4 (br, 7H, Ar). IR (cm^{-1}, KBr): 3444, 3056, 2954, 2866, 1721, 1599, 1492, 1456, 1420, 1385, 1330, 1258, 1200, 1114, 1039, 978, 885, 820, 761, 742, 722.

3. Results and discussion

3.1. Monomer synthesis

Scheme 2 illustrates the synthetic routes for monomers **1**–**4**. They were synthesized by the reaction of menthyl and bornyl chloroformates with 2- and 3-trimethylsilylethynylcarbazoles, followed by desilylation using TBAF. The structures of the monomers were confirmed by IR, ^{1}H, and ^{13}C NMR spectra besides elemental analysis.

3.2. Polymerization

Table 1 summarizes the conditions and results of the polymerization of carbazole-containing monomers catalyzed by (nbd)$Rh^+[\eta^6$-$C_6H_5B^-(C_6H_5)_3]$ in CH_2Cl_2 with the initial monomer concentration of 0.10 M at 30 °C for 24 h. The pale yellow polymerization mixture became orange within 3 min, and gradually turned dark orange with increasing viscosity. After a set time, the polymerization mixture was poured into a large amount of acetone to precipitate powdery polymers with moderate molecular weights (M_n: 11.5×10^3–92.2×10^3) in good yields (77–89%). Poly(**1**)–poly(**3**) were completely soluble in CH_2Cl_2, $CHCl_3$, toluene, THF, and insoluble in acetone, methanol, diethyl ether and *n*-hexane. Intriguingly, however, poly(**4**) was completely soluble in $CHCl_3$ and THF but partly soluble in toluene and CH_2Cl_2 (80% of the polymer was soluble at the concentration of 0.3 g/dL). Raising the initial monomer concentration higher than 0.10 M resulted in the formation of solvent-insoluble polymers, presumably because the molecular weights became too high to dissolve in solvents. We also examined the polymerization in $CHCl_3$, THF, and toluene to find whether the obtained polymers were insoluble in organic solvents, even when the initial monomer concentration was 0.10 M. Interestingly, the $[(nbd)RhCl]_2$–Et_3N catalyst gave solvent-insoluble polymers even with the initial monomer concentration of 0.10 M in CH_2Cl_2. It seems that the solubility of the present polymers delicately depends upon the molecular weights and/or stereoregularity. We also polymerized the monomers using $MoCl_5$/*n*-Bu_4Sn and WCl_6/Ph_4Sn as catalysts in toluene at 30 °C for 24 h to obtain only low-molecular-weight oligomers ($M_n < 3000$).

3.3. Polymer structure

The polymer structures were examined by IR and ^{1}H NMR spectroscopies. The monomers exhibited IR absorption bands at around 3260 and 2100 cm^{-1} associated with the ≡C–H and –C≡C– stretching vibrations, respectively, while the polymers did not exhibit these peaks as shown in Fig. 1. Accordingly, the polymers displayed no ^{1}H NMR signal at around 3.0 ppm assignable to an acetylenic proton as exemplified for poly(**1**) in Fig. 2. All these results clearly indicated that the acetylene polymerization took place to form the polymers composed of alternating single and double bonds. The ^{1}H NMR signals of the polymers appeared very broadly,

Table 1
Polymerization of **1**–**4** by (nbd)$Rh^+[\eta^6$-$C_6H_5B^-(C_6H_5)_3]$[a]

Run	Monomer	Yield[b] (%)	$M_n \times 10^{-3}$ [c]	M_w/M_n [c]	Color
1	**1**	87	57.5	2.96	Yellow-orange
2	**2**	86	41.7	4.23	Yellow-orange
3	**3**	89	92.2	2.60	Red-brown
4	**4**	77	11.5	2.54	Pale yellow

[a] $[M]_0 = 0.10$ M, $[M]_0/[Rh] = 100$, in CH_2Cl_2, 30 °C, 24 h.
[b] Acetone-insoluble part.
[c] Determined by GPC in THF on the basis of polystyrene calibration.

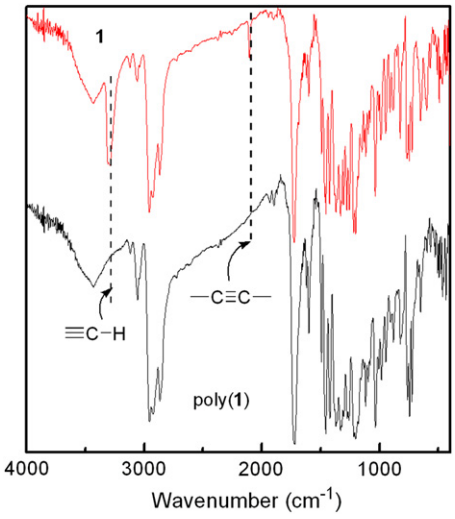

Fig. 1. IR spectra of **1** and poly(**1**).

and the signals assignable to the olefinic proton of the polyacetylene main chain overlapped with aromatic proton signals. It was therefore impossible to determine the *cis*/*trans* ratio of the main chain by ^{1}H NMR spectroscopy. Since Rh catalysts predominantly afford polyacetylenes with *cis*-stereoregular structure [8], it is assumed that the steric structure of the polymers in the present study is also the case. We also measured the ^{13}C NMR spectra of the polymers in addition to the IR and ^{1}H NMR spectra, but the signals were very broad, and gave no useful information on the polymer structure.

3.4. Secondary structure of the polymers

Table 2 summarizes the specific rotations ($[\alpha]_D$) of poly(**1**)–poly(**4**) along with the data of the monomers measured in $CHCl_3$, THF, toluene, and CH_2Cl_2 at room temperature. The $[\alpha]_D$ values of the polymers were much larger than those of their corresponding monomers in all the solvents except poly(**3**); e.g., the $[\alpha]_D$ of poly(**1**) in $CHCl_3$ (−1301°) was 12-fold larger than that of **1** (−109°). This suggests that poly(**1**), poly(**2**), and poly(**4**) take a regulated higher order structure such as helix with an excess of preferred handedness. These polymers showed larger $[\alpha]_D$ values in $CHCl_3$ and THF than that in toluene and CH_2Cl_2. Considering the dielectric constants of these solvents ($CHCl_3$ 4.8, THF 7.4, toluene 2.4, CH_2Cl_2 8.9), it seems that there is no clear correlation between the specific rotation and solvent polarity. Monomers **1** and **2** showed the same absolute $[\alpha]_D$ values with opposite signs. On the other hand, poly(**1**) and poly(**2**) showed different $[\alpha]_D$ values with opposite signs, presumably caused by the difference in molecular weights and/or stereoregularity. The $[\alpha]_D$ of poly(**1**) and poly(**2**) changed according to the solvent to a greater extent in magnitude than that of the monomers. Although **1** and **3** showed nearly the same $[\alpha]_D$, poly(**1**) and poly(**3**) showed very different $[\alpha]_D$. The substitution position of carbazole of the monomers did not affect the $[\alpha]_D$ so much, while it largely affected the conformation of polyacetylene backbone, resulting in the large difference in $[\alpha]_D$.

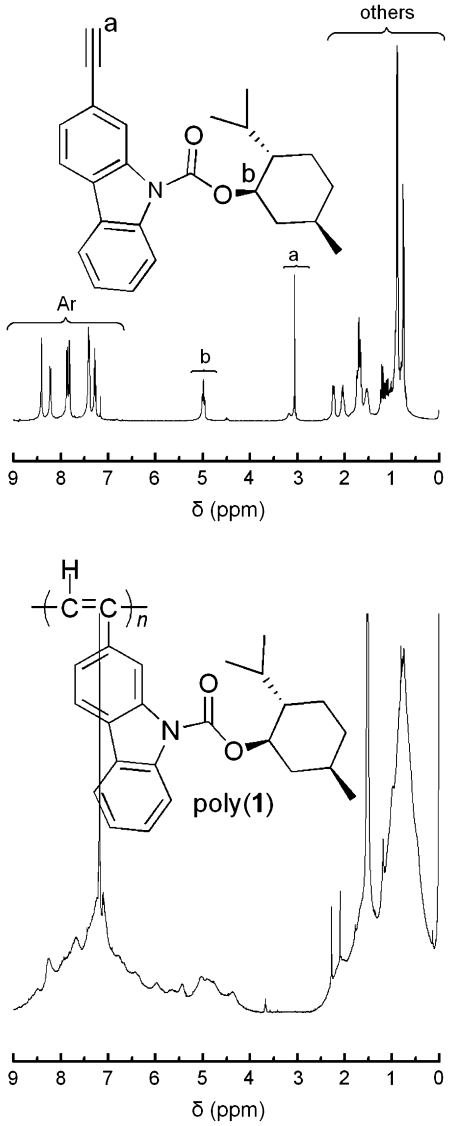

Fig. 2. ^{1}H NMR spectra of **1** and poly(**1**).

As discussed above, the large $[\alpha]_D$ values of the polymers imply that they take a helical conformation. We conducted CD spectroscopic analysis of polymer solutions to confirm the helicity. The top part of Fig. 3 shows the CD spectra of

Table 2
Optical rotations of **1**–**4** and poly(**1**)–poly(**4**)

Compound	$[\alpha]_D$[a] (°)			
	$CHCl_3$	THF	Toluene	CH_2Cl_2[b]
1	−109	−89	−85	−88
Poly(**1**)	−1301	−920	−288	−430
2	+109	+88	+85	+88
Poly(**2**)	+647	+882	+303	+264
3	−99	−67	−68	−70
Poly(**3**)	−63	−62	−40	−64
4	−4	−7	−3	−3
Poly(**4**)	−262	−180	−121	−132

[a] Measured by polarimetry ($c = 0.1$ g/dL).
[b] All the polymers were completely soluble in CH_2Cl_2 at a concentration of 0.1 g/dL.

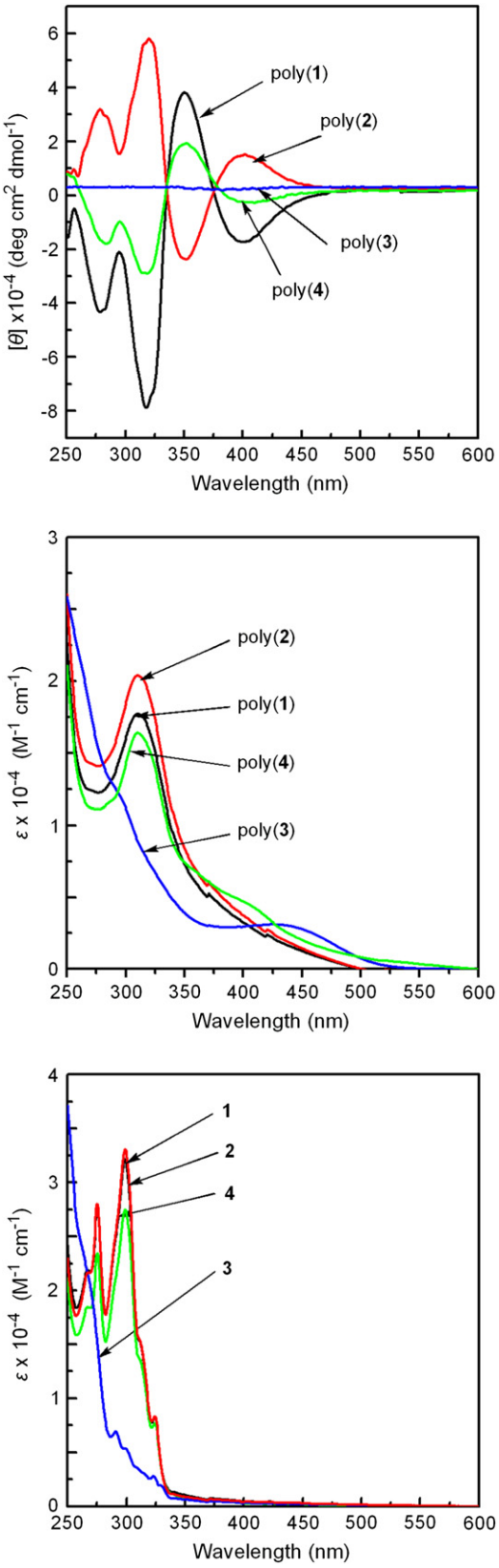

Fig. 3. CD and UV–vis spectra of poly(**1**)–poly(**4**) along with **1**–**4** measured in THF ($c = 1.34 \times 10^{-4}$ M) at 22 °C.

poly(**1**)–poly(**4**) measured in THF. Although monomers **1**–**4** were CD inactive (not shown), poly(**1**), poly(**2**), and poly(**4**) showed strong Cotton effects at 275, 320, 350, and 400 nm, unambiguously proving that the polymers adopted a helical conformation with a preferred screw sense. Poly(**1**) and poly(**2**) displayed mirror-imaged CD spectral patterns. Namely, poly(**1**) exhibited three large minus signals at 275, 320 and 400 nm, and a large plus CD signal at 350 nm, while poly(**2**) exhibited the CD signals with the opposite signs at the same wavelengths. The polymers exhibited absorption peaks at longer wavelength than the corresponding monomers as shown in the middle and bottom parts in Fig. 3. The UV–vis absorption peaks of the monomers at around 260–300 nm were attributable to carbazole. The band edges of the polymers extend to 500–600 nm, which should result from the conjugation of the polyacetylene main chain. Judging from the comparison between the UV–vis absorption spectra of the monomers and polymers, it seems that the helical polyacetylene main chain mainly induces the Cotton effects at around 350 and 400 nm, and helically arrayed carbazole units induce the ones at around 275 and 320 nm. Poly(**4**) exhibited CD and UV–vis spectral pattern similar to those of poly(**1**) and poly(**2**). On the other hand, poly(**3**) exhibited no Cotton effect, which agreed with the small $[\alpha]_D$ compared with those of the others.

The CD intensities of the polymers largely depended on the solvent, which agreed with the different specific rotations according to the solvent as summarized in Table 2. Fig. 4 depicts the solvent dependence of CD and UV–vis spectra of poly(**2**) as an example. It is noteworthy that the intensities of UV–vis absorption at 310 nm were almost the same irrespective of the solvent. Consequently, it is considered that the degree of one handedness of helicity changes according to the solvent.

The significant dependence of the CD spectra on solvents was also observed in mixed solvents of $CHCl_3$ and methanol with various compositions as shown in Fig. 5. As the methanol content increased, the magnitude of the CD signals at 275 and 320 nm remarkably decreased, while a minimal change was observed in the CD and UV–vis spectra at 350–500 nm. These results indicate the different origins of the observed optical activity at different methanol compositions. We also measured CD and UV–vis spectra of the polymer solutions after filtration with a membrane having the pore size of 0.45 μm. No change was found before and after filtration at methanol compositions of 40% and less. On the other hand, the polymer solutions with methanol compositions of 60 and 80% remarkably decreased the intensities of the CD and UV–vis signals after filtration, the CD intensities of the signals became ca. 1/10 and almost zero after filtration, respectively. It is concluded that the polymers formed aggregates upon addition of methanol [15]. As described above, it is likely that the CD signals at 275 and 320 nm originate from helically arrayed carbazole side chains, and those of 350 and 400 nm originate from the polyacetylene backbone. It is assumed that the helical carbazole array became disordered to decrease the CD intensities at the shorter wavelength region due to aggregation upon methanol addition, while the main chain kept the helicity, leaving the CD signals at the longer

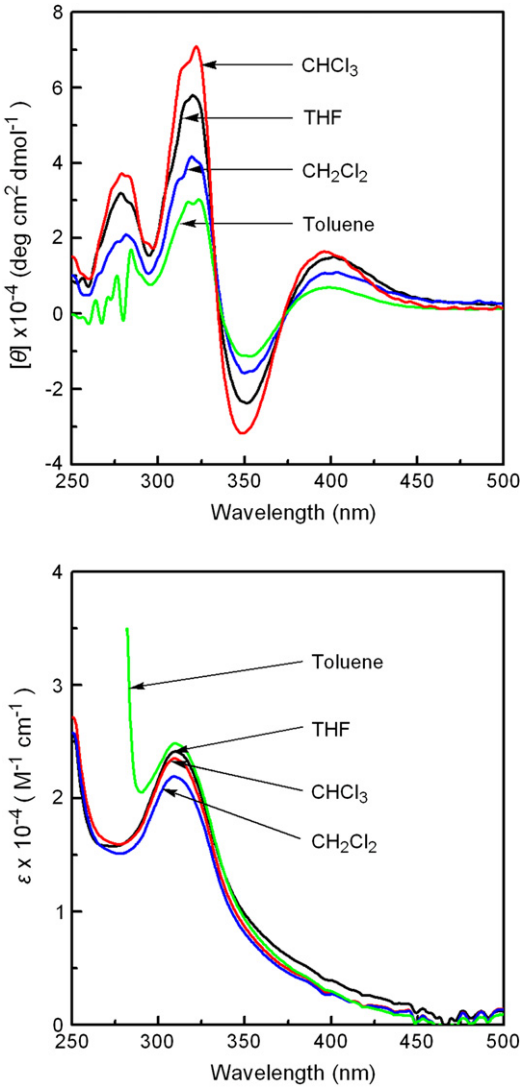

Fig. 4. CD and UV–vis spectra of poly(**2**) measured in $CHCl_3$, THF, toluene, and CH_2Cl_2 ($c = 1.34 \times 10^{-4}$ M) at 22 °C.

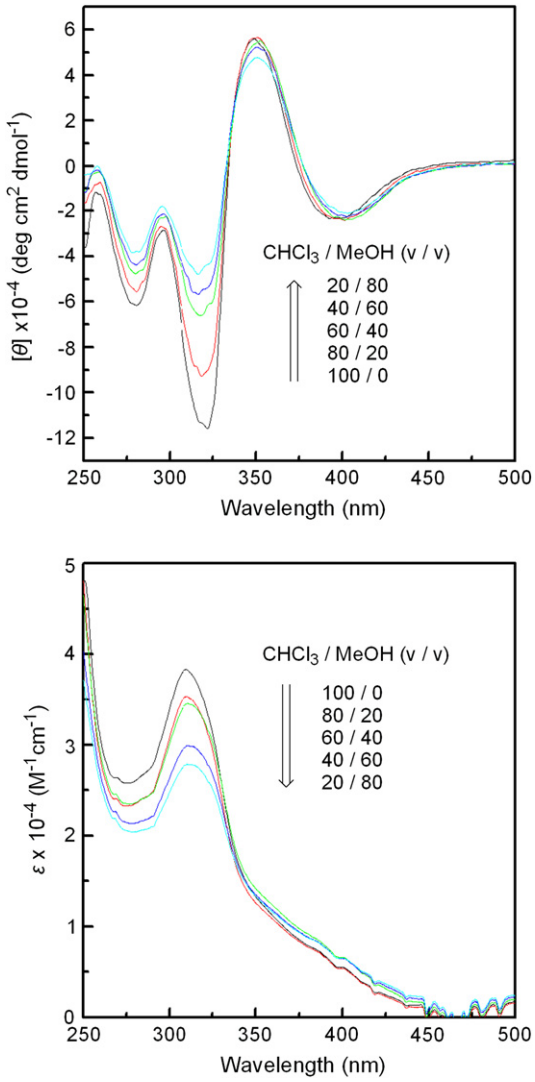

Fig. 5. CD and UV–vis spectral changes of poly(**1**) measured in $CHCl_3$–methanol ($c = 1.34 \times 10^{-4}$ M) with various compositions (100/0–20/80, v/v) at 20 °C.

wavelength region intact. It is noteworthy that disordering of the helical array of the carbazole pendants caused no change in the helicity of the polyacetylene backbone, but the concrete reason is unclear.

Fig. 6 depicts the temperature dependence of the CD and UV–vis spectra of poly(**1**) and poly(**2**) measured in $CHCl_3$. When the measuring temperature was raised from −10 to 40 °C, the magnitude of Cotton effect only slightly changed. The helical structure of the polymers was thermally stable at this temperature range. The UV–vis absorption maxima of poly(**1**) and poly(**2**) were observed at around 320 nm. The helical structure of poly(**4**) was also thermally stable similarly with those of poly(**1**) and poly(**2**), which was also confirmed by temperature-variable CD spectroscopic measurement.

3.5. Fluorescence properties

Fig. 7 shows the fluorescence spectra of poly(**1**)–poly(**4**). The polymer solution emitted luminescence, whose maximum wavelength was located at 370 nm upon excitation at 310 nm. The fluorescence quantum yields (ϕ) of the polymers were smaller than those of the corresponding monomers (ϕ of **1**, **2**, **3**, **4** were 22.0%, 24.3%, 21.8%, 7.7%, respectively). The reason may be associated with the differences in the chain stereoregularity and/or packing arrangements of the polymers in solution. The polyacetylene backbones are generally quenching sites for light emission. The polymer strand may absorb most of the light emitted from the appendages with the energy dissipated via nonradiative decay, thus resulting in low photoluminescence efficiency in the polymers. The fluorescence quantum yields of poly(**1**), poly(**2**) and poly(**4**) were larger than that of poly(**3**).

3.6. Electrochemical properties

Fig. 8 depicts the cyclic voltammetric (CV) curves of poly(**1**)–poly(**4**). Poly(**4**) exhibited an obvious oxidation peak

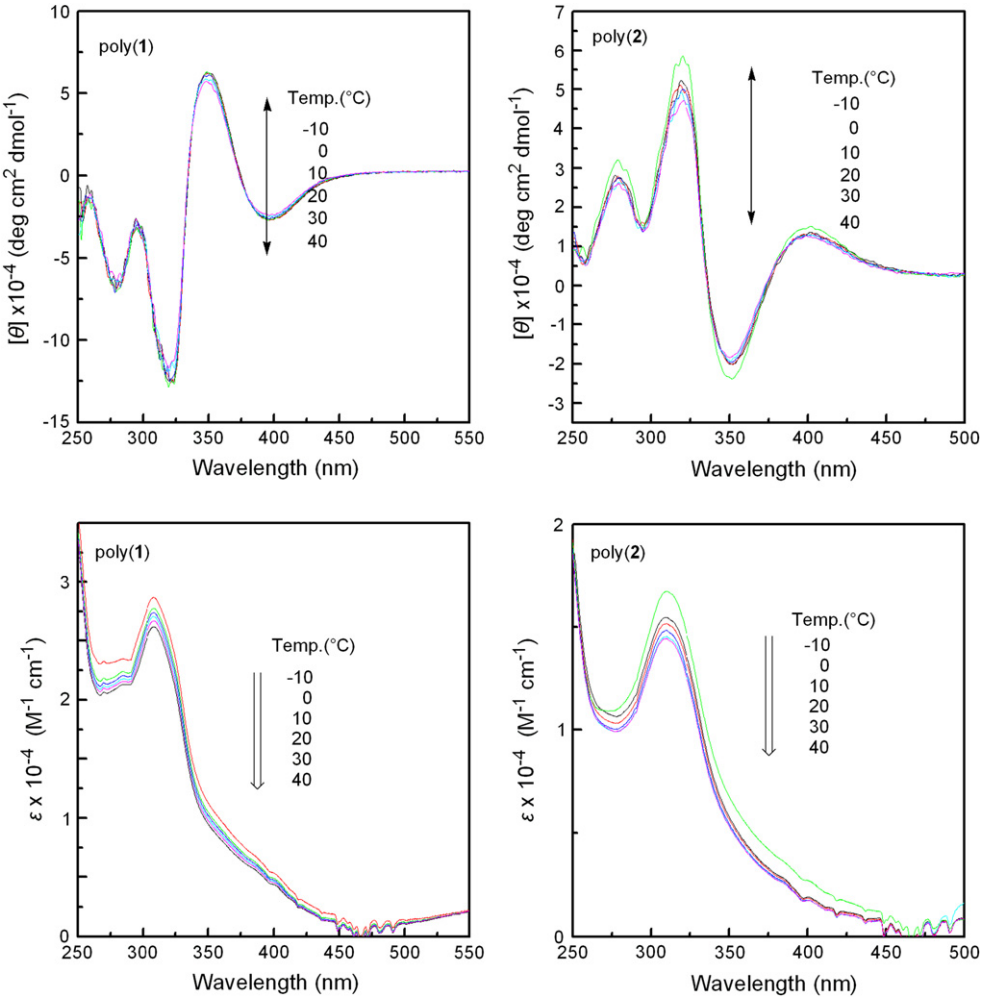

Fig. 6. CD and UV–vis spectral changes of poly(**1**) and poly(**2**) from −10 to 40 °C measured in $CHCl_3$ ($c = 1.00 \times 10^{-4}$ M).

at 1.10 V in the first scan, and shifted the peak to a higher potential field as the CV scans continued. It seems that a conducting polymer film was formed on the working electrode surface, and the film thickness gradually increased upon CV scanning. The potential shift of this maximum provided the information on the increase of the electrical resistance in the polymer film. Over-potential was presumably needed to overcome the resistance. The potential was somewhat higher than those of *N*-alkyl-substituted carbazole derivatives reported so far (0.7–0.8 V) [16]. On the other hand, poly(**1**)–poly(**4**) showed a clear reduction peak at about 0.65 V indicating that the present polymers exhibit obvious electrochemical properties.

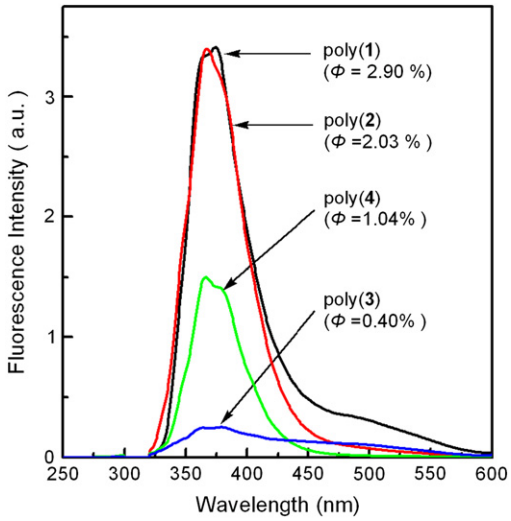

Fig. 7. Fluorescence spectra of poly(**1**)–poly(**4**) measured in CH_2Cl_2 ($c = 1.34 \times 10^{-5}$ M), excited at 310 nm. The intensities are normalized based on the concentrations of carbazole unit.

3.7. Thermal stability

Fig. 9 depicts the TGA traces of the polymers. The 5% weight loss temperatures were at around 310–330 °C under air, which were much higher than that of poly(phenylacetylene). The present polymers thermally degraded more slowly than poly(phenylacetylene) [17], which may be attributable to the bulky carbazole side chains. Poly(**3**) connecting carbazole at the 3-position lost its weight largely compared to poly(**1**) and poly(**2**) connecting carbazole at the 2-position at the temperature range from 350 to 550 °C. The substitution position affected the thermal decomposition behavior. Poly(**1**)

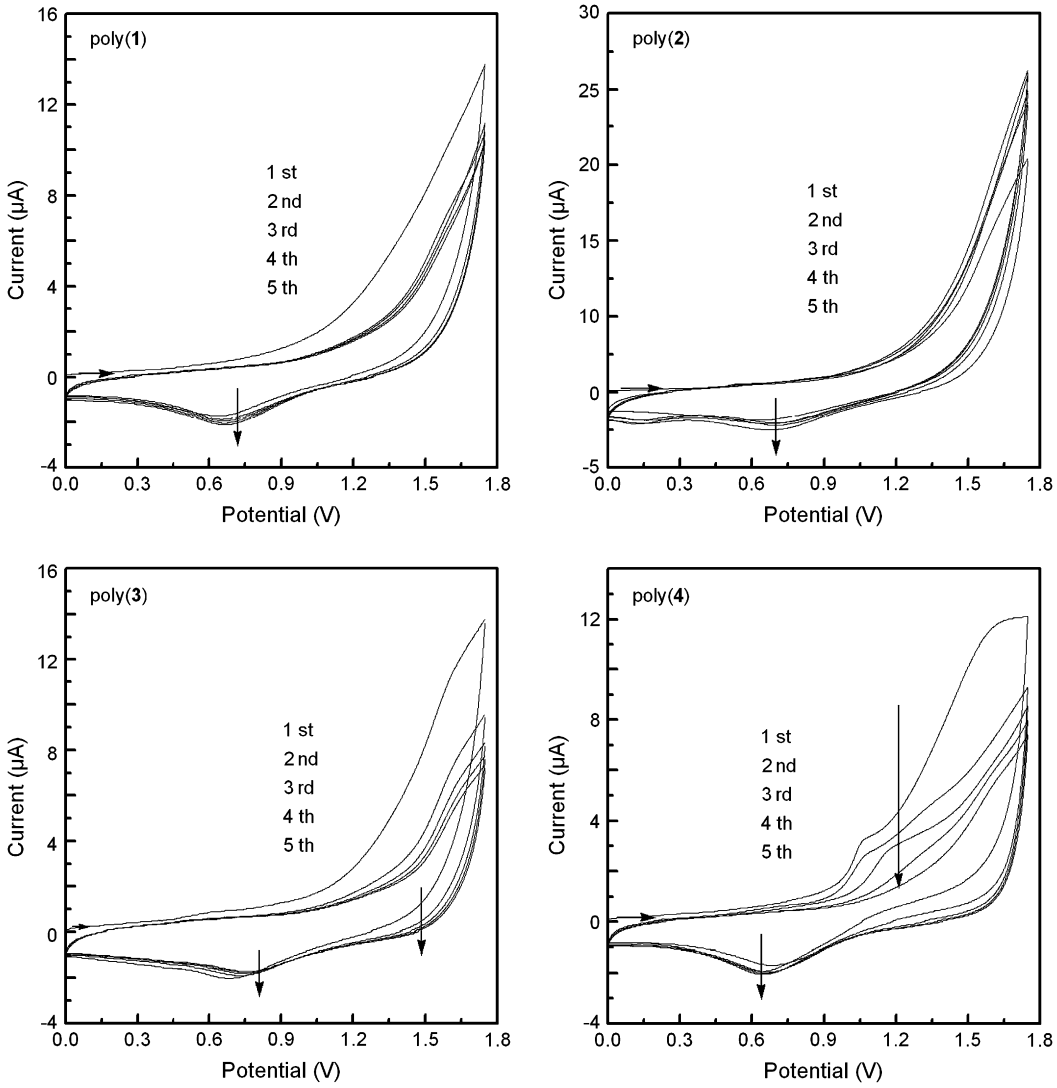

Fig. 8. Cyclic voltammograms of poly(**1**)–poly(**4**) measured at a scan rate of 0.1 V/s, vs Ag/Ag^{+} in a TBAP solution.

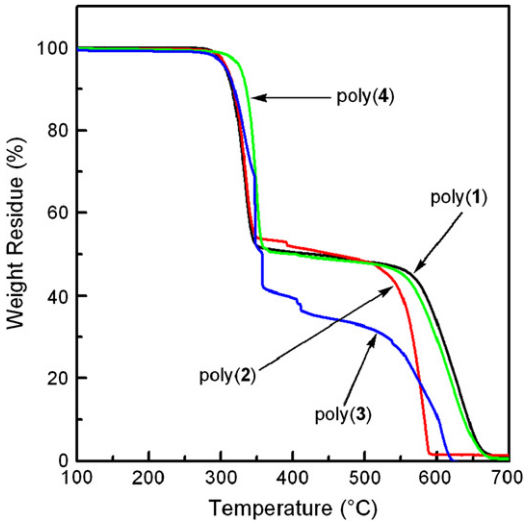

Fig. 9. TGA curves of poly(**1**)–poly(**4**) measured at a heating rate of 10 °C/min in air.

completely lost the weight at 660 °C, while the enantiomeric counterpart poly(**2**) did at 590 °C, presumably due to the lower molecular weight. The 5% weight loss temperature of borneol-derived poly(**4**) was ca. 20 °C higher than those of menthol-derived poly(**1**) and poly(**2**), suggesting that the thermal decomposition took place at the side chain in the first stage.

4. Conclusions

In this work, we have synthesized a group of acetylene derivatives **1**–**4** bearing carbazole moieties with different terminal groups, and polymerized them to obtain poly(**1**)–poly(**4**) with moderate molecular weights in good yields. Except poly(**3**), the polymers took a helical conformation with predominantly one-handed screw sense, exhibiting large molar ellipticities associated with the polyacetylene backbone and carbazole side chains; the Cotton effects at around

350 and 400 nm were assignable to the helical polyacetylene main chain, and those at around 275 and 320 nm were assignable to the carbazole rings oriented in a helical array. The signs of the optical rotations and molar ellipticities of poly(**1**) and poly(**2**) bearing (1*R*,2*S*,5*R*)- and (1*S*,2*R*,5*S*)-menthyl groups were opposite to each other. Upon addition of methanol to solutions of poly(**1**) and poly(**2**), the intensities of the CD signals based on polyacetylene backbone did not change, while those assignable to carbazole moieties remarkably decreased due to the formation of aggregates. The helical structure of the polymers was very stable against heating. The polymers emitted small fluorescence, and showed electrochemical properties.

Acknowledgments

This research was partly supported by a Grant-in-Aid for Science Research in a Priority Area "Super-Hierarchical Structures (No. 446)" from the Ministry of Education, Culture, Sports, Science and Technology, Japan. Jinqing Qu acknowledges the financial support from the Ministry of Education, Culture, Sports, Science, and Technology (Monbukagakusho), Japan.

References

[1] (a) Wang YZ, Epstein AJ. Acc Chem Res 1999;32:217;
(b) Grazulevicius JV, Strohriegl P, Pielichowski J, Pielichowski K. Prog Polym Sci 2003;28:1297.
[2] (a) Jack W, Lam Y, Tang BZ. Acc Chem Res 2005;38:745;
(b) Nagai K, Masuda T, Nakagawa T, Freeman BD, Pinnau I. Prog Polym Sci 2001;26:721;
(c) Masuda T. Acetylenic polymers. In: Salamone JC, editor. Polymeric material encyclopedia, vol. 1. New York: CRC; 1996. p. 32.
[3] (a) Okamoto Y, Nakano T. Chem Rev 1994;94:349;
(b) Nakano T, Okamoto Y. Chem Rev 2001;101:4013.
[4] (a) Yuki H, Okamoto Y, Okamoto I. J Am Chem Soc 1980;102:6356;
(b) Okamoto Y, Honda S, Okamoto I, Yuki H, Murata S, Noyori R, et al. J Am Chem Soc 1981;103:6971;
(c) Okamoto Y, Hatada K. J Liq Chromatogr 1986;9:369;
(d) Huang WS, Hu QS, Zhang XF, Andrerson J, Pu L. J Am Chem Soc 1997;117:4313;
(e) Yashima E, Maeda K, Okamoto Y. Polym J 1999;31:1033.
[5] Aoki T, Kokai M, Shinohara K, Oikawa E. Chem Lett 1993;2009.
[6] Yashima E, Huang S, Matsushima T, Okamoto Y. Macromolecules 1995; 28:4184.
[7] (a) Li BS, Cheuk KKL, Salhi F, Lam JWY, Cha JAK, Xiao X, et al. Nano Lett 2001;1:323;
(b) Li BS, Cheuk KKL, Ling LS, Chen JW, Xiao XD, Bai CL, et al. Macromolecules 2003;36:77;
(c) Li BS, Cheuk KKL, Yang D, Lam JWY, Wan LJ, Bai C, et al. Macromolecules 2003;36:5447;
(d) Cheuk KKL, Lam JWY, Chen J, Lai LM, Tang BZ. Macromolecules 2003;36:5947;
(e) Cheuk KKL, Lam JWY, Lai LM, Dong YP, Tang BZ. Macromolecules 2003;36:9752.
[8] (a) Nomura R, Fukushima Y, Nakako H, Masuda T. J Am Chem Soc 2000;122:8830;
(b) Nomura R, Tabei J, Masuda T. J Am Chem Soc 2001;123:8430;
(c) Nomura R, Nishiura S, Tabei J, Sanda F, Masuda T. Macromolecules 2003;36:5076;
(d) Sanda F, Araki H, Masuda T. Macromolecules 2005;38:10605;
(e) Tabei J, Shiotsuki M, Sanda F, Masuda T. Macromolecules 2005; 38:9448;
(f) Gao G, Sanda F, Masuda T. Macromolecules 2003;36:3938.
[9] (a) Tang BZ, Chen HZ, Xu RS, Lam JWY, Cheuk KKL, Wong HNC, et al. Chem Mater 2000;12:213;
(b) Pui-Sze Lee P, Geng Y, Kwok HS, Tang BZ. Thin Solid Films 2000; 363:149.
[10] Tabata M, Fukushima T, Sadahiro Y. Macromolecules 2004;37:4342.
[11] (a) Onishi K, Advincula RC, Abdul Karim SM, Nakai T, Masuda T. ACS Polym Prepr 2002;43(1):171;
(b) Nakano M, Masuda T, Higashimura T. Polym Bull 1995;34:191;
(c) Sata T, Nomura R, Wada T, Sasabe H, Masuda T. J Polym Sci Part A Polym Chem 1998;36:2489;
(d) Sanda F, Kawaguchi T, Masuda T. Macromolecules 2003;36:2224;
(e) Sanda F, Nakai T, Kobayashi N, Masuda T. Macromolecules 2004; 37:2703;
(f) Sanda F, Kawasaki R, Shiotsuki M, Masuda T. Polymer 2004; 45:7831;
(g) Qu J, Kawasaki R, Shiotsuki M, Sanda F, Masuda T. Polymer 2006; 47:6551.
[12] Fulghum T, Abdul Karim SM, Baba A, Taranekar P, Nakai T, Masuda T, et al. Macromolecules 2006;39:1467.
[13] Sanda F, Kawasaki R, Shiotsuki M, Takashima T, Fujii A, Ozaki M, et al., submitted for publication.
[14] Percec V, Obata M, Rudick JG, De BB, Glodde M, Bera TK, et al. J Polym Sci Part A Polym Chem 2002;40:3509.
[15] (a) Bouchard J, Belletête M, Durocher G, Leclerc M. Macromolecules 2003;36:4624;
(b) Belletête M, Bouchard J, Leclerc M, Durocher G. Macromolecules 2005;38:880.
[16] Wei ZH, Xu JK, Nie GM, Du YK, Pu SZ. J Electroanal Chem 2006; 589:112;
(b) Chiu KY, Su TX, Li JH, Lin TH, Liou GS, Cheng SH. J Electroanal Chem 2005;575:95.
[17] Nakai T, Karim SMA, Teraguchi M, Sanda F, Masuda T. J Macromol Sci Pure Appl Chem 2002;A39:935.